Genes & Diseases (2022) 9, 140–150

Available online at www.sciencedirect.com

ScienceDirect

journal homepage: http://ees.elsevier.com/gendis/default.asp

FULL LENGTH ARTICLE

Lysyl oxidase inhibition enhances browning of white adipose tissue and adaptive thermogenesis

Chun Xing [1], Duo Jiang [1], Yang Liu, Qiqun Tang, Haiyan Huang*

Key Laboratory of Metabolism and Molecular Medicine, The Ministry of Education, Department of Biochemistry and Molecular Biology, Fudan University School of Basic Medical Sciences, Shanghai 200032, PR China

Received 4 August 2020; received in revised form 24 September 2020; accepted 5 October 2020
Available online 10 October 2020

KEYWORDS
Adaptive thermogenesis;
BAT;
Beige fat;
Lysyl oxidase;
TNFα

Abstract Accumulating evidence from both animal and human studies suggests that activation of beige fat increases cellular energy expenditure, ultimately reducing adiposity. Here, we report the central role of adipocyte-derived lysyl oxidase (Lox) in the formation of thermogenic beige fat. Mice exposed to cold or a β3 agonist showed drastically lower Lox expression in thermogenically activated beige fat. Importantly, inhibition of Lox activity with BAPN stimulated biogenesis of beige fat in inguinal white adipose tissue (iWAT) under housing conditions and potentiated cold-induced adaptive thermogenesis and beiging in both iWAT and epididymal white adipose tissue (eWAT). Notably, white adipocytes with Lox repression undergo transdifferentiation into beige adipocytes which can be suppressed by tumor necrosis factor-α (TNFα) via ERK activation. This work provides new insight into the molecular control to expand beige fat by Lox inhibition and suggest the potential for utilizing inhibitor of Lox to treat the emerging epidemics of obesity and diabetes.

* Corresponding author. Fax: +86 21 64033738.
E-mail address: haiyanhuang@shmu.edu.cn (H. Huang).
Peer review under responsibility of Chongqing Medical University.
[1] Contribute equally to this paper.

https://doi.org/10.1016/j.gendis.2020.10.001

Introduction

Obesity, defined as an excess in fat mass, predisposes individuals to multiple metabolic diseases.[1–3] White adipose tissue (WAT) and brown adipose tissue (BAT) represent traditionally recognized adipose types, with WAT functioning primarily as storage for excess energy. In contrast, BAT specializes in dissipating energy via induction of uncoupling protein 1 (Ucp1) during cold- or diet-induced thermogenesis, making BAT a potential target for anti-obesity therapeutics. Recently, a third type, the beige/brite adipocyte, has been identified within WAT that is distinct from the "classical" brown adipocyte.[4]

Beige adipocytes localize to various WAT depots.[5–9] Under basal conditions, these cells show a white adipocyte-like phenotype and lack Ucp1 expression. However, in response to chronic cold exposure[10] or β3-adrenergic activators,[11] these cells convert into brown-like adipocytes that express Ucp1 and display small, multilocular lipid droplets.

Beige adipocytes are either derived from a population of beige preadipocytes[4,12] or are converted from white adipocytes by specific stimuli.[13,14] Multiple secretory factors, such as fibroblast growth factor-21 (FGF21),[6] the cardiac peptides (ANP/BNP),[15] irisin,[16,17] bone morphogenetic protein 4 (BMP-4),[18] meteorin-like protein (Metrnl),[19] and adiponectin,[20] are capable of inducing WAT browning.

The immune system has been recently implicated in this browning process. Specifically, the type 2 cytokines interleukin (IL)-4/13 and alternative activation of macrophages within WAT can trigger browning via the release of catecholamines.[21] A more recent study identified a critical role for IL-33-activated type 2 innate lymphoid cells (ILC2s) in the regulation of beige fat biogenesis.[22,23] Additionally, the cytokine IL-6 is required for a full induction of Ucp1 in response to cold exposure and exercise.[24] In contrast, the proinflammatory cytokine tumor necrosis factor-α (TNF-α) has been shown to suppress the transformation of white adipocytes into brown-like adipocytes.[25] Ongoing research will rapidly expand the list of browning agents.

Lysyl oxidase (Lox), a copper-dependent amine oxidase, is synthesized as a preproLox protein that undergoes post-translational modifications to yield the 50-kDa glycosylated pro-Lox, which is eventually proteolytically processed by bone morphogenetic protein-1 (BMP-1)[26] and other proteinases[27] to separate the propeptide from the mature Lox enzyme. Lox primarily catalyzes the covalent cross-linking of collagens and elastin within the extracellular matrix (ECM).[28] More recently, Lox has been identified as a regulator of various pathologies, including cancer and inflammation.[29,30]

We have previously demonstrated that Lox participates in the commitment of pluripotent stem cells to the adipocytic lineage.[31] Recent reports also showed that Lox is upregulated in adipose tissue from obese individuals, rats fed a high-fat diet, and ob/ob mice.[32,33] However, the physiological relevance and the underlying mechanisms whereby Lox participates in biogenesis of beige fat remain undefined. Here, we report that a critical role for Lox in the remodeling of WAT into thermogenic beige fat. We determined that Lox inhibition drives conversion of white adipocytes into beige adipocytes which can be suppressed by TNFα.

Materials and methods

Animal studies

Mice were housed in a controlled environment (12 h light/dark cycle, 60—70% humidity). For cold challenge experiments, 5-week-old male mice were housed in pre-chilled cages at 4 °C for 3 days. For CL316243 administration, 5-week-old male C57BL/6J mice were given daily i.p. injections of CL316243 (0.5 mg/kg body weight/day) or saline for 4 days. For BAPN administration, BAPN (100 mg/kg/day; Sigma—Aldrich, St Louis, MO, USA) or PBS i.p. injections were initiated 1 day prior to cold exposure and then mice were housed in pre-chilled cages at 4 °C for 3 days.

All studies were approved by the Animal Care and Use Committee of Fudan University School of Basic Medical Sciences and followed the National Institute of Health guidelines on the care and use of animals.

Generation of TG mice overexpressing adipose-specific Lox-EGFP

Adipose-specific Lox-EGFP transgene (Lox-EGFP TG) mice were generated at Model Animal Research Center of Nanjing University. To generate Lox-EGFP TG mice carrying the Lox-EGFP fusion protein specifically overexpressed in adipose tissue, fragments of 5.4-kb adipocyte protein-2 (aP2) promoter was first amplified,[34] and inserted into the pInsulator vector. The newly constructed vector was named pInsulator-aP2. DNA fragments encoding Lox (GenBank accession NM_001286181.1), EGFP and a flexible linker (GGGGSGGGGSGGGGS) inserted between Lox AND EGFP were amplified by PCR with high-fidelity DNA polymerase and ligated into pInsulator-aP2 vector by SLIC. The final vector was reconfirmed by PCR, enzyme digestion and sequencing before shooting into zygotes. Mice carrying the transgene were identified by PCR analysis of genomic DNA from tail snips using the following paired primers that specifically detect the transgene but not endogenous Lox: TGTCTCCTCCACAATGAGGCA (forward primer 1); GCCCGTTGTTCTCCCATTGG (reverse primer 1) or GGCATCGACTTCAAGGAGGA (forward primer 2), AGCCAGAAGTCAGATGCTCAA (reverse primer 2).

Indirect calorimetry

Whole-body oxygen consumption was monitored using a comprehensive laboratory animal monitoring system (CLAMS, Columbus Instruments). Mice were housed singly in metabolic cages, acclimated for 48 h, and monitored. Data on oxygen consumption rate (VO_2, mL/kg/h) was recorded at 25 min intervals throughout the 48 h period.

Rectal temperature

A mouse rectal Microprobe Thermometer (Physitemp Instruments Inc.) was used to examine body temperature when needed.

Histologic analysis

Tissues were fixed in 4% paraformaldehyde for at least 48 h, embedded in paraffin, and cut into 5-μm sections. Sections were stained with hematoxylin and eosin (H&E) or incubated with rabbit anti-Ucp1 antibody (Abcam, ab23841) for immunohistochemical analysis.

Cell culture and induction of adipogenesis

3T3-L1 preadipocytes were plated at low density and cultured in DMEM containing 10% (vol/vol) calf serum. Two days postconfluence (designated day 0), cells were induced to differentiate with DMEM containing 10% (vol/vol) FBS, 1 μg/mL insulin (I), 1 μM dexamethasone (D), and 0.5 mM 3-isobutyl-1-methyl-xanthine (M) for 2 days. Cells were then treated with DMEM supplemented with 10% (vol/vol) FBS and 1 μg/mL insulin for 2 days, after which DMEM containing 10% (vol/vol) FBS was refreshed every other day. Adipocyte gene expression and acquisition of an adipocyte phenotype is maximal by day 8. For the induction of beige adipocytes, C3H10T1/2 cells were first committed to preadipocyte and then induced to differentiate as described before.[35]

Isolation of adipocytes and stromal vascular fraction from whole adipose tissue

Adipose tissue was dissected, washed in PBS, minced, and digested for 50 min at 37 °C in 0.1% (w/v) collagenase type VIII (Sigma—Aldrich, St. Louis, MO) with gentle shaking. Tissue suspensions were passed through a 100-μm cell strainer and centrifuged at 500 g for 5 min to pellet the SVF. The floating adipocytes were transferred to a fresh tube and the pellet containing SVFs was resuspended with ammonium chloride lysis buffer to remove red blood cells. Lysis buffer containing 50 mM Tris—HCl (pH 6.8), 2% SDS, phosphatase inhibitors (10 mM Na_3VO_4 and 10 mM NaF), and a protease inhibitor mixture (Roche Applied Science) was added to the pellet containing SVF or transferred adipocyte fraction for protein extraction. Equal amounts of protein were subjected to SDS-PAGE and immunoblotted using specific primary antibodies.

RNA interference

Lox-specific stealth siRNA duplexes (GCGGAUGUCAGAGACUAUGACCACA) were designed and synthesized by Invitrogen (Invitrogen, Carlsbad, CA). Stealth siRNA negative control duplexes had a similar GC content. Fully differentiated 3T3-L1 adipocytes (day 8) were transfected with siRNA duplexes using Lipofectamine RNAi MAX according to the manufacturer's instructions (Invitrogen, Carlsbad, CA). For TNFα treatment, 20 ng/mL of purified recombinant TNFα (PeproTech) was added to the medium from day 9 through day 11.

Adenoviral expression vectors and infection

To generate mature-Lox-EGFP (Ma-Lox-EGFP) adenoviral expression vectors, mouse cDNA of mature Lox with signal peptide was first cloned into pEGFP-N3 using the following primers: GAAGATCTATGCGTTTCGCCTGGGCTGT (forward primer); CGCGGATCCATACGGTGAAATTGTGC AGCCT (reverse primer). The above vector was then used as a template for the construction of adenoviral expression vector pAd/CMV/V5-DEST (Invitrogen, Carlsbad, CA, USA) encoding Ma-Lox-EGFP according to the manufacturer's protocol. Adenovirus was amplified in the 293A cells and subsequently purified using CsCl density gradient centrifugation.

In vitro oxygen consumption in differentiated adipocytes

Oxygen consumption was measured using the XF96 extracellular flux analyzer (Agilent). Briefly, 5×10^3 3T3-L1 preadipocytes were plated in XF96-well cell culture plate. Following differentiation, 3T3-L1 adipocytes were treated with Stealth siRNA negative control or Lox-specific stealth siRNA for 48 h. Afterwards, cells were subjected to the mitochondrial stress test by adding 1 μM oligomycin followed by 1 μM carbonyl cyanide4-(trifluoromethoxy) phenylhydrazone (FCCP) and 1.5 μM antimycin/rotenone.

Western blot

WAT, BAT or cultured cells were homogenized in lysis buffer containing 50 mM Tris-HCl (pH 6.8), 2% SDS, phosphatase inhibitors (10 mM Na_3VO_4 and 10 mM NaF), and a protease inhibitor mixture (Roche Applied Science, Mannheim, Germany). Equal amounts of protein were subjected to SDS-PAGE and immunoblotted using specific primary antibodies: anti-Lox and anti-Hsp 90 (Santa Cruz Biotechnology, CA, USA); anti-Ucp1 and anti-Pgc1α (Abcam, Cambridge, UK); anti-ERK1/2 and anti-p-ERK1/2.

Real-time quantitative PCR

Total RNA was isolated using TRIzol reagent. PrimeScript RT Master Mix (TaKaRa) and random primers were used for first strand cDNA synthesis. Real-time quantitative PCR was carried out using a 2 × PCR Master Mix (Power SYBR Green; Applied Biosystems), specific primer sequences (Table S1) and an Applied Biosystems 7300 Real-Time PCR System. Results were normalized using 18S rRNA.

Lipid detection using Nile Red staining

In vitro differentiated 3T3-L1 adipocytes were characterized using Dye Nile Red (Sigma—Aldrich) and DAPI according to the manufacturer's instructions. Briefly, 3T3-L1 adipocytes were incubated in PBS with Nile Red (stock: 0.5 mg/mL in acetone, final: 0.5 μg/mL) for 5 min. Images were obtained using a confocal microscope (Leica TCS SP5).

Lipid detection using Oil Red O staining

In vitro differentiated 3T3-L1 adipocytes were washed 3 times with PBS and then fixed for 10 min with 3.7% formaldehyde. Oil Red O (0.5% in isopropanol) was diluted with

water (3:2), filtered through a 0.45-μm filter, and incubated with the fixed cells for 1 h at room temperature. The cells were then washed with water and the stained fat droplets in the adipocytes were visualized by light microscopy and photographed.

Statistical analyses

Two-tailed Student's *t*-tests were used to compare groups with respect to continuous variables. Quantile-quantile plots were used to examine the distributions of the variables of interest. All data from samples are reported as the mean ± SEM. Differences were considered significant at $^{*}P < 0.05$, $^{**}P < 0.01$, and $^{***}P < 0.001$.

Results

Lox in adipose tissue is down-regulated in response to thermogenic activation

To investigate the role of Lox in cold-induced thermogenic activation, mice were housed at 22 °C or 4 °C for 3 days. Western blot revealed that three days of cold exposure induced browning of WAT and activation of BAT as indicated by elevated Ucp1 expression (Fig. 1A–C). By contrast, there was an obvious decrease in Lox protein in iWAT, eWAT and BAT from cold-challenged mice (Fig. 1A–C). This change was accompanied by a modest decline in serum Lox of mice challenged with cold exposure (Fig. 1D). To recapitulate cold exposure, we next investigated the effects of the β3-adrenergic agonist CL316243 on Lox expression in mouse adipose tissue. We confirmed that CL316243 also induced Ucp1 expression and decreased Lox protein expression in both iWAT and BAT (Fig. 1E, F). These findings demonstrated that Lox in adipose tissue is down-regulated in response to thermogenic activation.

Improved thermogenic activity in mice with pharmacological inhibition of Lox

To explore whether decreased Lox is sufficient for thermogenic activity, BAPN, an irreversible and specific inhibitor of Lox activity was used.[36] Under housing temperature (22 °C) or thermoneutral temperature (30 °C), mouse rectal temperatures and body weight were not affected by BAPN injection (Fig. S1A–D). Of note, when housed at a cold temperature, the mice injected with BAPN had higher rectal temperatures and energy expenditure than control mice (Fig. 2A–C), while no

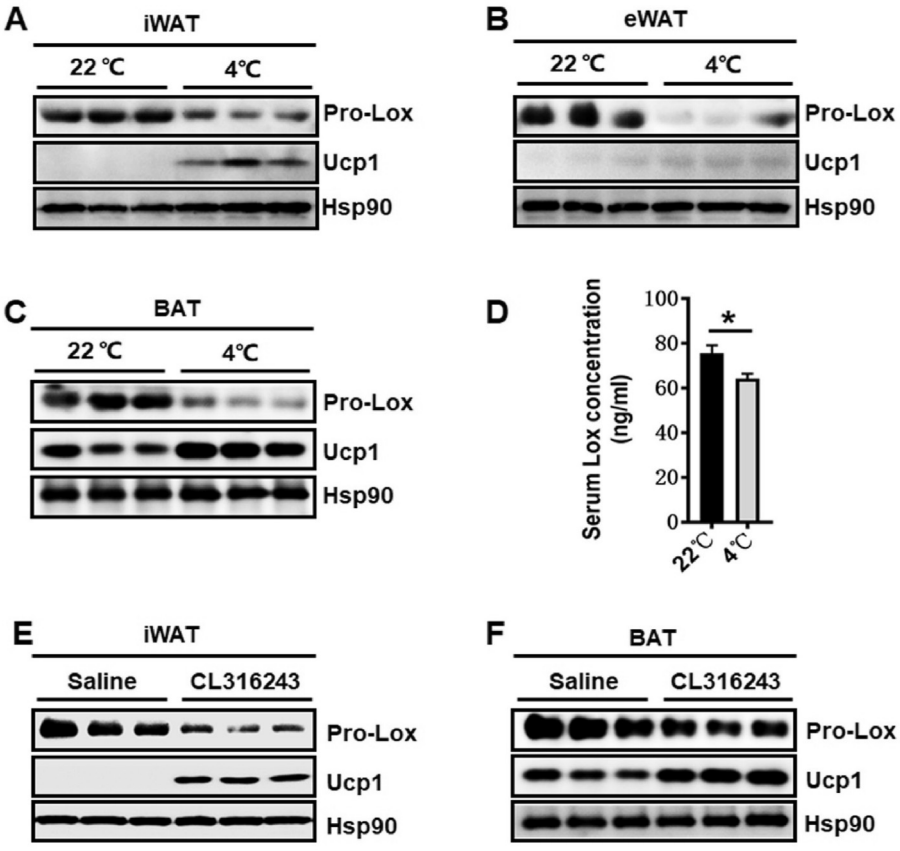

Figure 1 Lox is decreased in response to thermogenic activation. **(A–D)** 5-week-old C57BL/6J mice were housed at 4 °C for 3 days or at 22 °C as control. Western blot analysis for Lox and Ucp1 in iWAT **(A)**, eWAT **(B)** and BAT **(C)**. **(D)** ELISA analysis for serum Lox level. **(E, F)** 5-week-old C57BL/6J mice were injected daily with CL316243 (1 mg/kg b.w.) or saline for 4 days. Western blot analysis of Lox and Ucp1 expression in iWAT **(E)** and BAT **(F)**. Data are presented as the mean ± SEM. $^{*}P < 0.05$ (Two-tailed Student's *t* test).

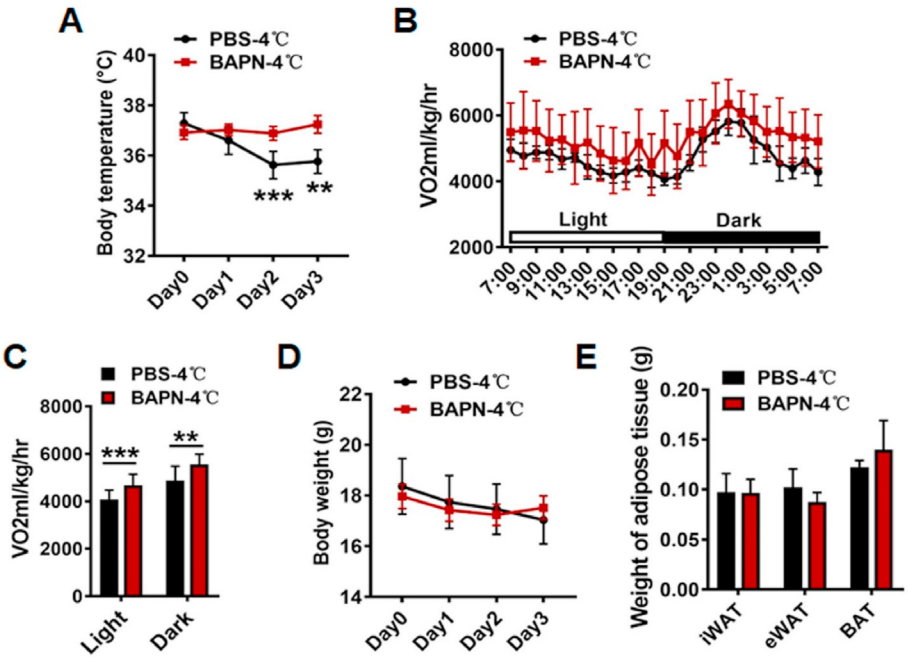

Figure 2 Pharmacological inhibition of Lox with BAPN promotes adaptive thermogenesis. 5-week-old C57BL/6J mice treated with PBS or BAPN were housed at 4 °C for 3 days ($n = 5$ each). **(A)** Rectal temperature of mice treated with PBS or BAPN. **(B, C)** Changes in whole-body oxygen consumption of mice treated with PBS or BAPN **(B)** over a 24 h period and **(C)** during one day/light cycle. **(D)** Changes in body weight for PBS- and BAPN-treated mice upon cold challenge. **(E)** The relative weight of adipose tissue. Data are presented as the mean ± SEM. $^{*}P < 0.05$, $^{**}P < 0.01$, $^{***}P < 0.001$ (Two-tailed Student's *t* test).

obvious change in body weight and adipose tissue weight was observed (Fig. 2D, E).

Pharmacological inhibition of Lox impairs thermogenic activity and enhances lipid accumulation in BAT

Since BAT specializes in energy expenditure through adaptive thermogenesis, we next investigate whether BAT activation contribute to Lox inhibition-induced higher energy expenditure. Surprisingly, cold-induced thermogenic activation of interscapular BAT of BAPN-treated mice was impaired, as indicated by lower expression of Ucp1 protein and mRNA level and other thermogenic genes, including *cidea* and *Zic1* (Fig. 3A, B). By contrast, genes implicated in lipid synthesis, such as *Acc1*, *Fasn* and *Srebp1c* and fatty acid transport related genes *Lpl* and *Cd36* were upregulated, while fatty acids oxidation gene *Cpt1* were dramatically decreased (Fig. 3C). Consistent with these observations, larger lipid droplets and lower level of epinephrine were observed in BAT of mice injected with BAPN (Fig. 3D—E), supporting the induction of a whitened phenotype in BAT of BAPN-treated mice with cold exposure. Taken together, these results demonstrated that Lox inhibition induced higher energy expenditure of cold exposed mice is not due to BAT activation.

Pharmacological inhibition of Lox promotes browning in white adipose tissue

Next, we tested whether beige fat contributes to the increased whole-body energy expenditure observed in BAPN-treated mice. Histologic analysis showed a greater abundance of multilocular adipocytes in the iWAT of BAPN-treated mice compared to control mice under either 22 °C or 4 °C (Fig. 4A, Fig. S2A). More Ucp1^{+} beiged adipocytes were observed in iWAT from cold-challenged mice with BAPN treatment (Fig. 4B). In addition, both Ucp1 and Pgc1α protein are induced by BAPN, which is negatively related to Lox protein level (Fig. 4C). BAPN administration also robustly increased in expression of key thermogenic genes and mitochondria genes, including *Ucp1*, *Cidea*, *Ebf3*, *Eva1*, *Elovl3*, and *Cox8b* in iWAT from mice under cold conditions (Fig. 4D). Conversely, mRNA levels of the white-specific gene *Hoxc9* and *Leptin* were considerably lower in iWAT from cold-exposed mice with BAPN administration (Fig. 4D). The upregulation of *Ucp1* expression by BAPN was also evident at 22 °C (Fig. S2B). More beige fat was also observed in epididymal white adipose tissue (eWAT) of BAPN treated-mice as indicated by smaller lipid droplets and increase in core set of thermogenic genes (Fig. 4E, F). It should be noted that fatty acids oxidation gene *Cpt1b* in both iWAT and eWAT from cold-exposed mice with BAPN treatment was significantly increase as well (Fig. 4G, H). Together, these data suggest that pharmacological inhibition of Lox promotes browning in white adipose tissue under both cold and housing conditions.

Disruption of Lox promotes browning of white adipocytes through transdifferentiation

Browning of white adipocytes can occur through either differentiation of WAT-resident precursor cells or "transdifferentiation" of white adipocytes. To uncover how Lox regulates the browning of WAT, stromal vascular fraction

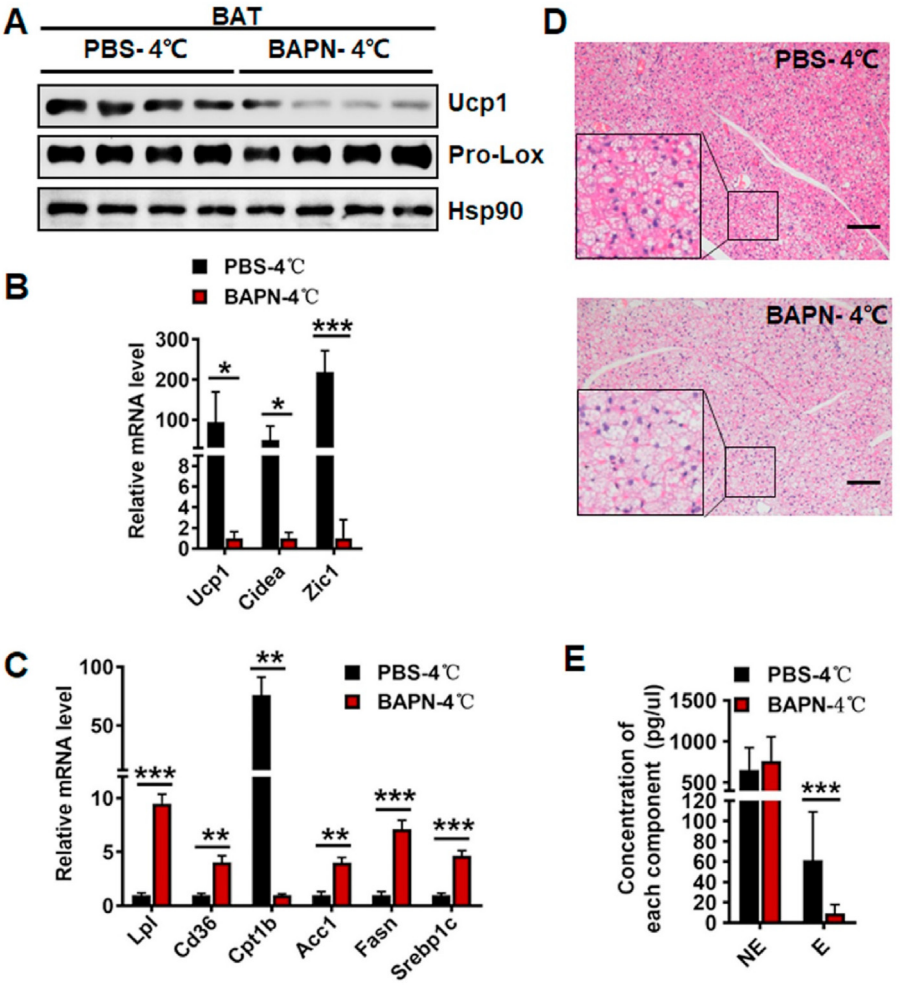

Figure 3 BAPN treatment enhances lipid accumulation and impairs thermogenic activity in BAT upon cold challenge. 5-week-old C57BL/6J mice treated with PBS or BAPN were housed at 4 °C for 3 days ($n = 5$ each). **(A)** Western blot analysis of BAT Ucp1 and Pgc1α protein expression. **(B)** BAT-specific genes expression within BAT. **(C)** Relative gene expression pattern of fatty acid transport, fatty acid oxidation and synthesis within BAT. **(D)** Representative images of H&E staining of BAT (scale bar, 100 μm). **(E)** Quantification of norepinephrine and epinephrine within BAT. Data are presented as the mean ± SEM. $^{*}P < 0.05$, $^{**}P < 0.01$, $^{***}P < 0.001$ (Two-tailed Student's *t* test).

(SVF) and mature adipocytes were isolated from iWAT or eWAT. Pro-Lox was predominantly present in mature adipocytes and barely detectable in SVF, whereas mature Lox was expressed both in SVF and adipocytes (Fig. 5A). Cold exposure led to a decrease in both Pro-Lox and mature Lox protein present in the adipocyte fractions (Fig. 5A). To investigate whether Lox contributes to the browning process, Lox was knocked down in white adipocytes that had been fully differentiated from 3T3-L1 preadipocytes. Both Ucp1 and Pgc1α protein level were elevated in the cells with Lox knockdown (Fig. 5B). The mRNA levels of key thermogenic genes (*Ucp1*, *Cidea*, *Eva1 and Elovl3*) and beige cell markers (*Cd137*, *Tmem26* and *Tbx1*) were significantly increased in cells with Lox knockdown (Fig. 5C). This was consistent with Lox knockdown adipocytes had greater basal and uncoupling oxygen consumption compared to control cells (Fig. 5D, E). Consistently, the accumulated lipid droplets were smaller in cells with *Lox* knockdown than that in control cells as determined by Nile red staining (Fig. 5F). Transmission electron microscopy further revealed healthier-looking mitochondria in cells following Lox knockdown, demonstrating a protective effect for mitochondria (Fig. 5G). We have also overexpressed Lox in beige adipocytes differentiated from C3H10T1/2 cells. Unsurprisingly, overexpression of Lox suppressed the expression of beige-related gene and key thermogenic genes (Fig. S3A–C). Moreover, the accumulated lipid droplets were larger in the Lox-overexpressed adipocytes than in controls as determined by Oil Red O staining (Fig. S3D). These findings collectively confirmed that Lox inhibition promotes browning of white adipocytes through transdifferentiation.

Downregulation of TNFα is required for the Lox inhibition-induced browning of white adipocytes

We next investigated the molecular mechanisms through which Lox regulates white adipocyte browning. Evaluation

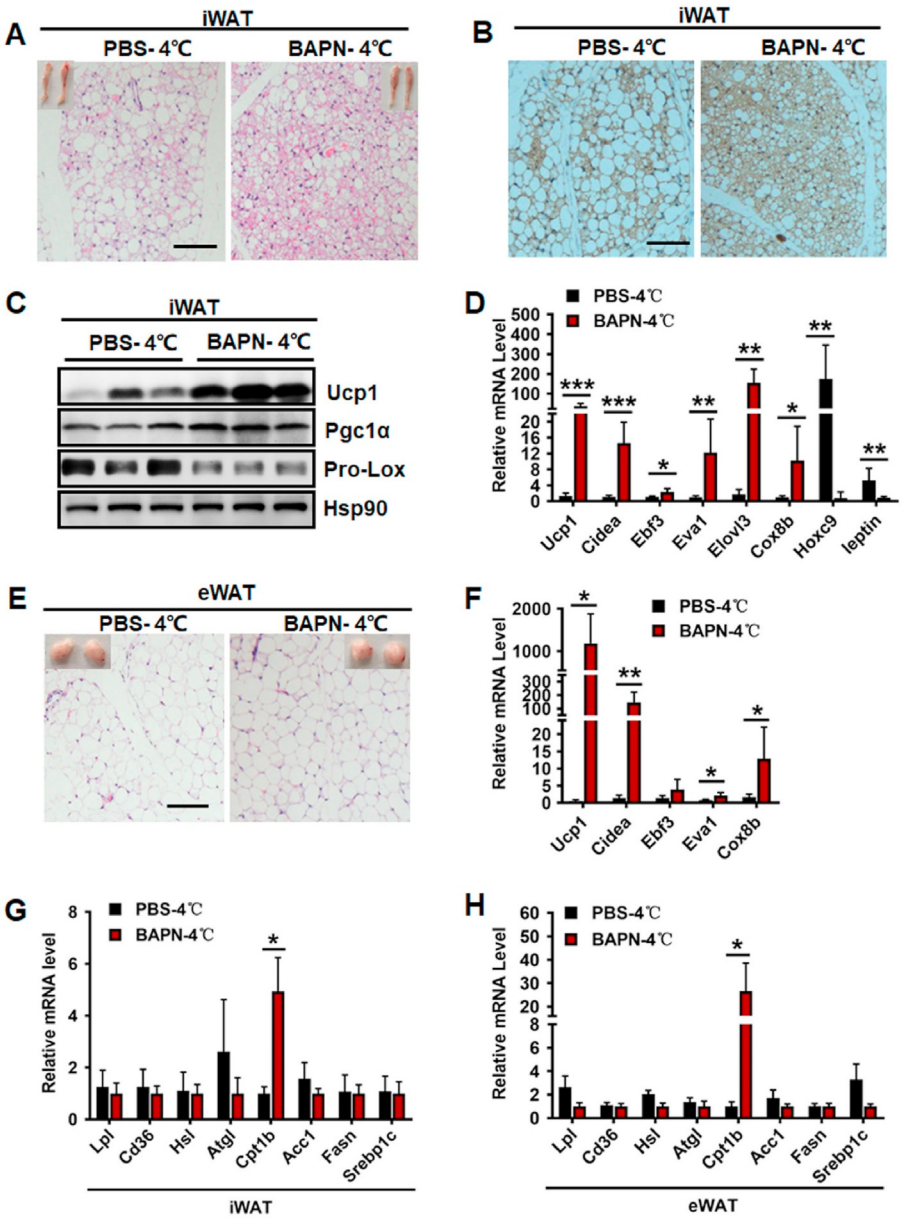

Figure 4 Pharmacological inhibition of Lox promotes browning of white adipose tissue in cold exposed mice. 5-week-old C57BL/6J mice treated with PBS or BAPN were housed at 4 °C for 3 days ($n = 5$ each). **(A)** Representative images of H&E staining of iWAT (scale bar, 100 μm). **(B)** Representative images of iWAT Ucp1 staining (scale bar, 100 μm). **(C)** Western blot analysis of iWAT Ucp1 and Pgc1α protein expression. **(D)** Expression of thermogenic genes and white-specific genes within iWAT. **(E)** Representative images of H&E staining of eWAT (scale bar, 100 μm). **(F)** Expression of thermogenic genes in eWAT. **(G, H)** Relative gene expression pattern of fatty acid transport, fatty acid oxidation and synthesis within iWAT and eWAT. Data are presented as the mean ± SEM. $^{*}P < 0.05$, $^{**}P < 0.01$, $^{***}P < 0.001$ (Two-tailed Student's *t* test).

of TNFα, a beiging suppressor via ERK activation,[25] revealed that *Tnfα* was repressed in iWAT of BAPN-treated mice with cold exposure and in fully differentiated 3T3-L1 adipocytes with Lox knockdown (Fig. 6A, B), suggesting that downregulation of TNFα might mediate the Lox inhibition-induced browning phenotype. To further address whether this phenotype is mediated by TNFα, *Lox* expression was knocked down in fully differentiated adipocytes derived from 3T3-L1 preadipocytes, followed by incubation with TNFα for 2 days. Expression of *Ucp1* and other key thermogenic genes were decreased with TNFα treatment (Fig. 6C, D). Consistently, Oil Red O staining showed that TNFα greatly increased the size of lipid droplets relative to the vehicle control (Fig. 6E). In addition, ERKs mediating the inhibitory effect of TNFα on the thermogenic marker is also suppressed in Lox knockdown cells (Fig. 6B, C). Furthermore, TNFα administration suppressed the BAPN-induced browning phenotype in mouse iWAT as indicated by less multilocular adipocytes and lower thermogenic gene expression without affecting

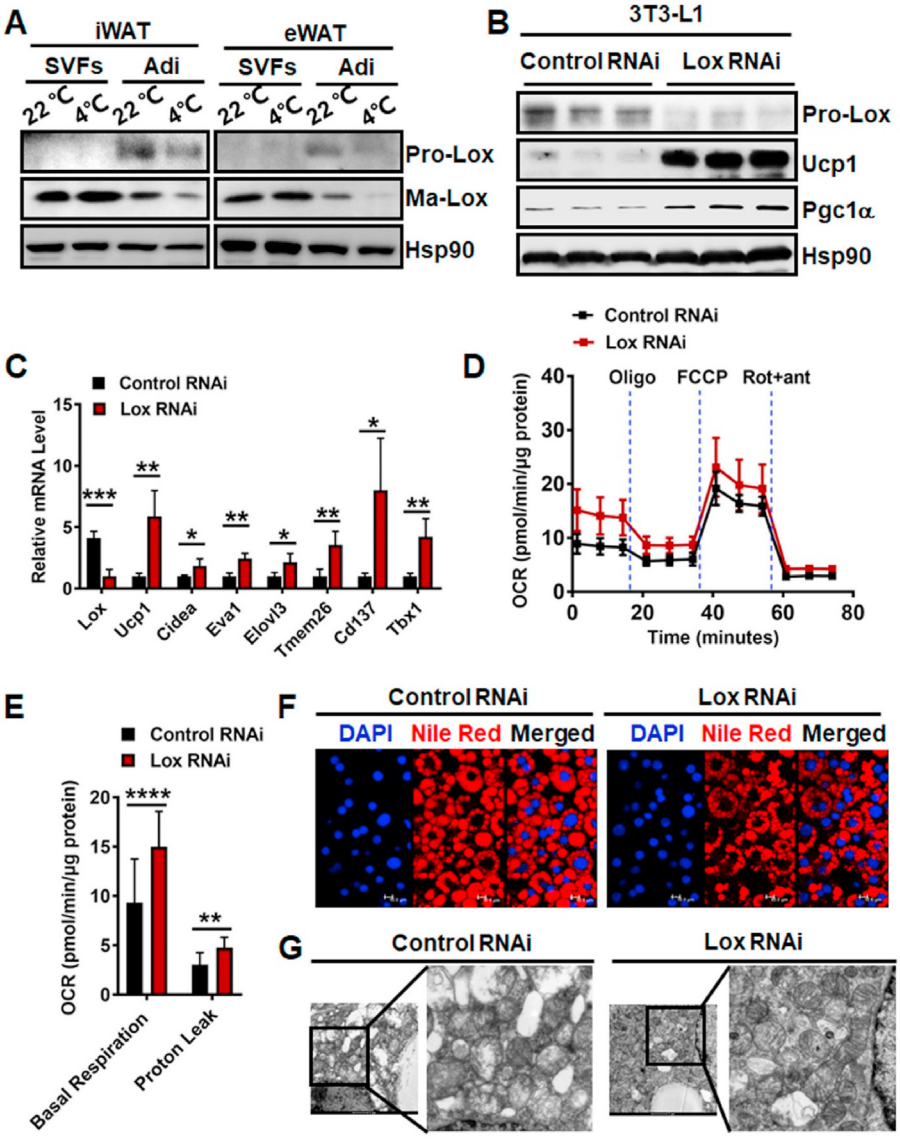

Figure 5 White adipocytes with Lox knock-down undergo transdifferentiation into beige adipocytes. **(A)** Western blot analysis of Lox protein expression in the stromal vascular fractions (SVFs) and adipocytes (Adi) of iWAT or eWAT from 5-week-old C57BL/6J male mice housed at 4 °C or 22 °C for 3 days. (B—G) Adipocytes fully differentiated from 3T3-L1 preadipocytes at day 8 after MDI induction followed by Lox knockdown for another 3 days. **(B)** Western blot analysis of Lox, Ucp1, and Pgc1α protein expression. **(C)** Expression of thermogenic genes and beige adipocyte-specific genes. **(D, E)** The Oxygen consumption rates of differentiated 3T3-L1 cells with or without Lox knock-down ($n = 5$/group). **(F)** Nile red staining. **(G)** Transmission electron microscopy showing mitochondrial morphology. Data are presented as the mean ± SEM. $^{*}P < 0.05$, $^{**}P < 0.01$, $^{***}P < 0.001$ (Two-tailed Student's t test).

body weight, iWAT weight and eWAT weight (Fig. 6F, G, S4A—D). Decreased Ucp1 and Pgc1α protein level has also been observed in iWAT from adipose tissue-specific Lox-EGFP TG mice with cold exposure (Fig. S5A). The size of inguinal adipocytes and fat droplets was increased in the Lox-EGFP TG mice as well (Fig. S5B). Consistently, elevated TNFα expression and activation of ERK signaling was observed in iWAT of the TG mice compared with WT mice (Fig. S5A, C). These results provided further evidence that the expression of a high level of Lox in WAT inhibits adipocyte browning *in vivo*.

Discussion

BAT dissipates chemical energy as heat through Ucp1 activity and increases energy expenditure.[37] Under certain conditions, white adipocytes can be partially converted into beige adipocytes that shares some features with brown adipocytes.[7—9] Increasing BAT activity or converting WAT adipocytes into beige adipocytes is considered a promising therapeutic strategy for combating obesity and metabolic diseases.[38—41] Several secretory factors, such as irisin,[16,17] FGF21,[6] meteorin-

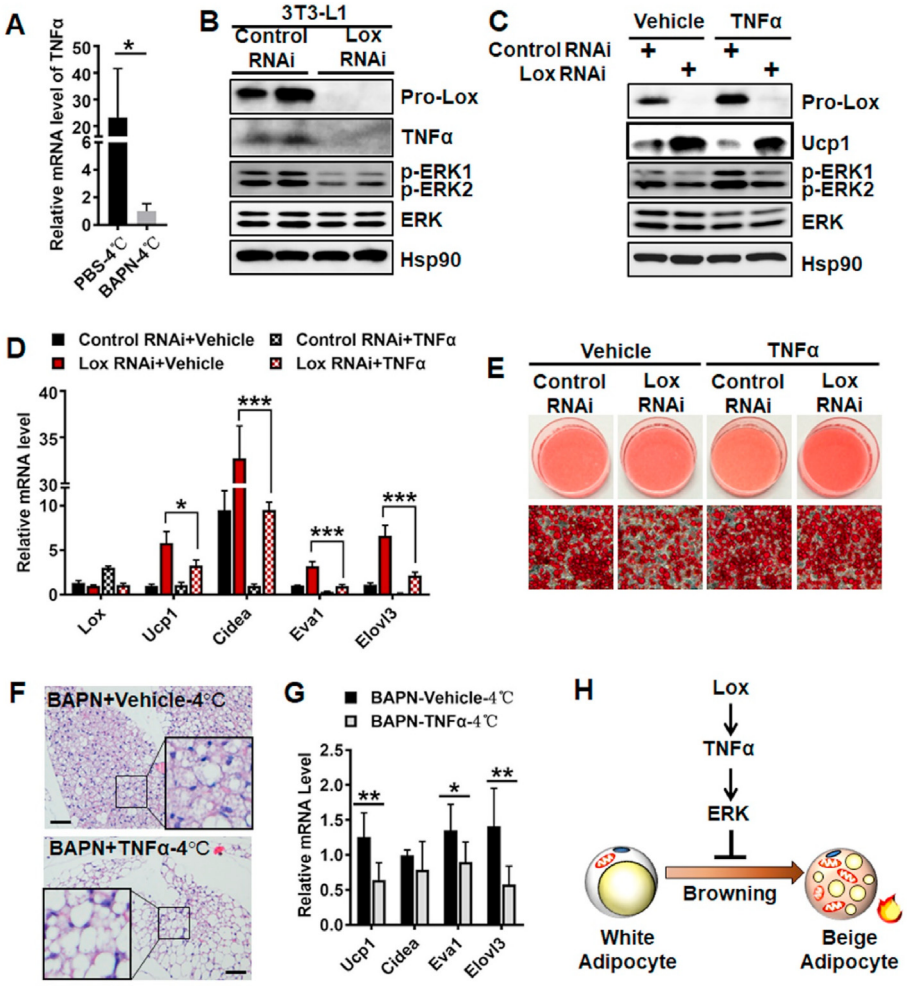

Figure 6 TNFα impairs the Lox inhibition-induced browning phenotype. **(A)** Real-time PCR analysis of TNFα mRNA expression in iWAT from 5-week-old C57BL/6J male mice housed at 4 °C with administration of PBS or BAPN for 3 days. **(B)** Effect of Lox knockdown on TNFα expression and ERK activation in adipocytes differentiated from 3T3-L1 preadipocytes. **(C)** Western blot analysis the effect of TNFα on Lox knockdown induced Ucp1 expression and ERK activation. **(D)** Real-time PCR analysis of relative mRNA expression, and **(E)** Oil Red O staining of lipid droplet in adipocytes fully differentiated from 3T3-L1 preadipocytes followed by Lox knockdown and TNFα administration. **(F)** Representative image of H&E staining of iWAT from BAPN-treated mice with/without TNFα administration (scale bar, 100 μm). **(G)** Real-time PCR analysis for relative mRNA expression in iWAT from BAPN-treated mice with/without TNFα administration. **(H)** Model of Lox inhibition inducing beige fat. Data are presented as the mean ± SEM. $^{*}P < 0.05$, $^{**}P < 0.01$, $^{***}P < 0.001$ (Two-tailed Student's *t* test).

like protein (Metrnl),[19] and adiponectin[20] are exclusive activators of beige cells.

Lox is a secreted, copper-dependent amine oxidase with a primary function of oxidizing amine substrates into reactive aldehydes, resulting in the crosslinking of collagen and elastin.[42–45] We demonstrate that cold exposure and β3 agonist, which activates the thermogenic program within adipocytes, lead to a markedly decrease in iWAT Lox expression (Fig. 1). Lox enzymatic activity is inhibited irreversibly by BAPN, which has been used in animal models in the context of tissue fibrosis or metastasis.[36] Here, we found that pharmacological inhibition of Lox by BAPN promotes the expression of browning marker Ucp1 in iWAT under housing conditions (22 °C) (Fig. 4). In a cold environment, BAPN administration greatly increased numbers of beige adipocytes in the inguinal fat pad compared to the vehicle control. Of note, in a cold environment, BAPN administration also significantly increased *Ucp1* expression in eWAT (Fig. 4), a type of WAT that is not as prone to produce beige adipocytes as is iWAT.[46] Our results clearly demonstrated that Lox inhibition in WAT leads to increased browning and whole-body energy expenditure regardless of the increased lipid accumulation in BAT and its reduced ability to oxidize lipids.

Crosstalk between BAT and WAT is an emerging research topic. It was reported that BAT expansion suppresses formation of beige adipocytes within iWAT.[47] In contrast, a paucity of BAT causes a compensatory induction of beige adipocytes in iWAT.[5] In addition, an ectopic WAT Ucp1 expression inhibits BAT Ucp1 expression.[48] Different regulation of thermogenic programming in BAT and WAT has also been observed in *Raptor* deficiency mice, *BMP4* transgene

mice and mice with increased circulating BMP4.[18,49,50] We also demonstrated that Lox inhibition induced more beige fat in WAT and decreased BAT activity in a cold environment (Fig. 2, 3), which might be partially explained by lower level of epinephrine in BAT of mice injected with BAPN. However, it is still unclear whether this opposite effect of BAPN on BAT and WAT is caused by a compensatory mechanism or not. Further studies are still needed to explore this.

The relative contributions of beige fat to whole body energy expenditure are not fully understood. In rodents, it is estimated that *in vivo* beige fat can only reach about 20% of the UCP1-dependent oxygen consumption per gram of tissue compared to that of canonical BAT.[41] We demonstrated that BAPN-induced iWAT and eWAT browning more than compensates for BAPN-induced BAT whitening as evidenced by much higher core body temperature and oxygen consumption (Fig. 2, 3). These data thus suggest that energy expenditure due to BAPN-induced browning of WAT far exceeds any negative impact on BAT. Given much of the fats observed in adult humans are white fats, targeting Lox to expand beige fat may be a reasonable strategy for treating obesity and metabolic diseases.

Several immune cytokines, including IL-4, IL-5, IL-6, and IL-13, have also been shown to promote browning process.[19,21–24] By contrast, TNFα, a well-known pro-inflammatory cytokine, was shown to inhibit Ucp1 expression via Erk activation.[25] Here, we demonstrated BAPN treatment decreases iWAT TNFα expression in cold exposed mice and Lox disruption inhibited TNFα expression in 3T3-L1 adipocytes. Furthermore, TNFα administration inhibited Lox disruption-induced browning both *in vitro* and *in vivo* in Erk-dependent manner (Fig. 6). However, the detailed mechanisms underlying the regulation of TNFα by Lox remains to be unraveled, but affecting chromatin organization,[51–53] acting as a transcriptional factor,[54,55] or regulating functions of cell surface receptors via its enzymic activity,[56] might be involved. In summary, we demonstrate that Lox is naturally repressed during thermogenic activation of beige fat. Lox inhibition potentiates white-to-brown conversion by suppressing TNFα (Fig. 6H).

Author contributions

Chun Xing: collection and assembly of data, data analysis and interpretation. Duo Jiang: collection of data and manuscript writing. Yang Liu: data analysis and interpretation. Qiqun Tang: data analysis and interpretation. Haiyan Huang: conception and design, data analysis and interpretation, financial support, manuscript writing and final approval of manuscript.

Conflict of interests

The authors declare no conflict of interest.

Funding

This research was supported by National Natural Science Foundation (No. 81770844, 82070870 and 81170781 to H.Y. Huang).

Appendix A. Supplementary data

Supplementary data to this article can be found online at https://doi.org/10.1016/j.gendis.2020.10.001.

References

1. Friedman JM. Obesity: causes and control of excess body fat. *Nature*. 2009;459(7245):340–342.
2. Heber D. An integrative view of obesity. *Am J Clin Nutr*. 2010;91(1):280S–283S.
3. Wisse BE, Kim F, Schwartz MW. Physiology. An integrative view of obesity. *Science*. 2007;318(5852):928–929.
4. Wu J, Bostrom P, Sparks LM, et al. Beige adipocytes are a distinct type of thermogenic fat cell in mouse and human. *Cell*. 2012;150(2):366–376.
5. Schulz TJ, Huang P, Huang TL, et al. Brown-fat paucity due to impaired BMP signalling induces compensatory browning of white fat. *Nature*. 2013;495(7441):379–383.
6. Fisher FM, Kleiner S, Douris N, et al. FGF21 regulates PGC-1alpha and browning of white adipose tissues in adaptive thermogenesis. *Genes Dev*. 2012;26(3):271–281.
7. Ohno H, Shinoda K, Spiegelman BM, Kajimura S. PPARgamma agonists induce a white-to-brown fat conversion through stabilization of PRDM16 protein. *Cell Metab*. 2012;15(3):395–404.
8. Seale P, Conroe HM, Estall J, et al. Prdm16 determines the thermogenic program of subcutaneous white adipose tissue in mice. *J Clin Invest*. 2011;121(1):96–105.
9. Frontini A, Vitali A, Perugini J, et al. White-to-brown transdifferentiation of omental adipocytes in patients affected by pheochromocytoma. *Biochim Biophys Acta*. 2013;1831(5):950–959.
10. Barbatelli G, Murano I, Madsen L, et al. The emergence of cold-induced brown adipocytes in mouse white fat depots is determined predominantly by white to brown adipocyte transdifferentiation. *Am J Physiol Endocrinol Metab*. 2010;298(6):E1244–E1253.
11. Himms-Hagen J, Melnyk A, Zingaretti MC, Ceresi E, Barbatelli G, Cinti S. Multilocular fat cells in WAT of CL-316243-treated rats derive directly from white adipocytes. *Am J Physiol Cell Physiol*. 2000;279(3):C670–C681.
12. Wang QA, Tao C, Gupta RK, Scherer PE. Tracking adipogenesis during white adipose tissue development, expansion and regeneration. *Nat Med*. 2013;19(10):1338–1344.
13. Rosenwald M, Perdikari A, Rulicke T, Wolfrum C. Bi-directional interconversion of brite and white adipocytes. *Nat Cell Biol*. 2013;15(6):659–667.
14. Ye L, Wu J, Cohen P, et al. Fat cells directly sense temperature to activate thermogenesis. *Proc Natl Acad Sci U S A*. 2013;110(30):12480–12485.
15. Bordicchia M, Liu D, Amri EZ, et al. Cardiac natriuretic peptides act via p38 MAPK to induce the brown fat thermogenic program in mouse and human adipocytes. *J Clin Invest*. 2012;122(3):1022–1036.
16. Bostrom P, Wu J, Jedrychowski MP, et al. A PGC1-alpha-dependent myokine that drives brown-fat-like development of white fat and thermogenesis. *Nature*. 2012;481(7382):463–468.
17. Villarroya F. Irisin, turning up the heat. *Cell Metab*. 2012;15(3):277–278.
18. Qian SW, Tang Y, Li X, et al. BMP4-mediated brown fat-like changes in white adipose tissue alter glucose and energy homeostasis. *Proc Natl Acad Sci U S A*. 2013;110(9):E798–E807.
19. Rao RR, Long JZ, White JP, et al. Meteorin-like is a hormone that regulates immune-adipose interactions to increase beige fat thermogenesis. *Cell*. 2014;157(6):1279–1291.

20. Hui X, Gu P, Zhang J, et al. Adiponectin enhances cold-induced browning of subcutaneous adipose tissue via promoting M2 macrophage proliferation. *Cell Metab*. 2015;22(2):279—290.
21. Qiu Y, Nguyen KD, Odegaard JI, et al. Eosinophils and type 2 cytokine signaling in macrophages orchestrate development of functional beige fat. *Cell*. 2014;157(6):1292—1308.
22. Lee MW, Odegaard JI, Mukundan L, et al. Activated type 2 innate lymphoid cells regulate beige fat biogenesis. *Cell*. 2015;160(1—2):74—87.
23. Brestoff JR, Kim BS, Saenz SA, et al. Group 2 innate lymphoid cells promote beiging of white adipose tissue and limit obesity. *Nature*. 2015;519(7542):242—246.
24. Knudsen JG, Murholm M, Carey AL, et al. Role of IL-6 in exercise training- and cold-induced UCP1 expression in subcutaneous white adipose tissue. *PLoS One*. 2014;9(1):e84910.
25. Sakamoto T, Takahashi N, Sawaragi Y, et al. Inflammation induced by RAW macrophages suppresses UCP1 mRNA induction via ERK activation in 10T1/2 adipocytes. *Am J Physiol Cell Physiol*. 2013;304(8):C729—C738.
26. Maruhashi T, Kii I, Saito M, Kudo A. Interaction between periostin and BMP-1 promotes proteolytic activation of lysyl oxidase. *J Biol Chem*. 2010;285(17):13294—13303.
27. Atsawasuwan P, Mochida Y, Katafuchi M, et al. A novel proteolytic processing of prolysyl oxidase. *Connect Tissue Res*. 2011;52(6):479—486.
28. Kagan HM, Li W. Lysyl oxidase: properties, specificity, and biological roles inside and outside of the cell. *J Cell Biochem*. 2003;88(4):660—672.
29. Cheng T, Liu Q, Zhang R, et al. Lysyl oxidase promotes bleomycin-induced lung fibrosis through modulating inflammation. *J Mol Cell Biol*. 2014;6(6):506—515.
30. Barker HE, Cox TR, Erler JT. The rationale for targeting the LOX family in cancer. *Nat Rev Cancer*. 2012;12(8):540—552.
31. Huang H, Song TJ, Li X, et al. BMP signaling pathway is required for commitment of C3H10T1/2 pluripotent stem cells to the adipocyte lineage. *Proc Natl Acad Sci U S A*. 2009;106(31):12670—12675.
32. Miana M, Galan M, Martinez-Martinez E, et al. The lysyl oxidase inhibitor beta-aminopropionitrile reduces body weight gain and improves the metabolic profile in diet-induced obesity in rats. *Dis Model Mech*. 2015;8(6):543—551.
33. Halberg N, Khan T, Trujillo ME, et al. Hypoxia-inducible factor 1alpha induces fibrosis and insulin resistance in white adipose tissue. *Mol Cell Biol*. 2009;29(16):4467—4483.
34. Ross SR, Graves RA, Greenstein A, et al. A fat-specific enhancer is the primary determinant of gene-expression for adipocyte-P2 in vivo. *Proc Natl Acad Sci U S A*. 1990;87(24):9590—9594.
35. Xue R, Wan Y, Zhang S, Zhang Q, Ye H, Li Y. Role of bone morphogenetic protein 4 in the differentiation of brown fat-like adipocytes. *Am J Physiol Endocrinol Metab*. 2014;306(4):E363—E372.
36. Bondareva A, Downey CM, Ayres F, et al. The lysyl oxidase inhibitor, beta-aminopropionitrile, diminishes the metastatic colonization potential of circulating breast cancer cells. *PLoS One*. 2009;4(5):e5620.
37. Smith RE. Thermoregulatory and adaptive behavior of Brown adipose tissue. *Science*. 1964;146(3652):1686—1689.
38. Wu J, Cohen P, Spiegelman BM. Adaptive thermogenesis in adipocytes: is beige the new brown? *Genes Dev*. 2013;27(3):234—250.
39. Harms M, Seale P. Brown and beige fat: development, function and therapeutic potential. *Nat Med*. 2013;19(10):1252—1263.
40. Kajimura S, Saito M. A new era in brown adipose tissue biology: molecular control of brown fat development and energy homeostasis. *Annu Rev Physiol*. 2014;76:225—249.
41. Shabalina IG, Petrovic N, de Jong JM, Kalinovich AV, Cannon B, Nedergaard J. UCP1 in brite/beige adipose tissue mitochondria is functionally thermogenic. *Cell Rep*. 2013;5(5):1196—1203.
42. Kagan HM, Trackman PC. Properties and function of lysyl oxidase. *Am J Respir Cell Mol Biol*. 1991;5(3):206—210.
43. Smith-Mungo LI, Kagan HM. Lysyl oxidase: properties, regulation and multiple functions in biology. *Matrix Biol*. 1998;16(7):387—398.
44. Lucero HA, Kagan HM. Lysyl oxidase: an oxidative enzyme and effector of cell function. *Cell Mol Life Sci*. 2006;63(19—20):2304—2316.
45. Xiao Q, Ge G. Lysyl oxidase, extracellular matrix remodeling and cancer metastasis. *Cancer Microenviron*. 2012;5(3):261—273.
46. Okamatsu-Ogura Y, Fukano K, Tsubota A, et al. Thermogenic ability of uncoupling protein 1 in beige adipocytes in mice. *PLoS One*. 2013;8(12):e84229.
47. Pan D, Mao C, Quattrochi B, et al. MicroRNA-378 controls classical brown fat expansion to counteract obesity. *Nat Commun*. 2014;5:4725.
48. Kopecky J, Clarke G, Enerback S, Spiegelman B, Kozak LP. Expression of the mitochondrial uncoupling protein gene from the aP2 gene promoter prevents genetic obesity. *J Clin Invest*. 1995;96(6):2914—2923.
49. Zhang X, Luo Y, Wang C, et al. Adipose mTORC1 suppresses prostaglandin signaling and beige adipogenesis via the CRTC2-COX-2 pathway. *Cell Rep*. 2021;34(9):108794.
50. Hoffmann JM, Grunberg JR, Church C, et al. BMP4 gene therapy in mature mice reduces BAT activation but protects from obesity by browning subcutaneous adipose tissue. *Cell Rep*. 2017;20(5):1038—1049.
51. Li W, Nellaiappan K, Strassmaier T, Graham L, Thomas KM, Kagan HM. Localization and activity of lysyl oxidase within nuclei of fibrogenic cells. *Proc Natl Acad Sci U S A*. 1997;94(24):12817—12822.
52. Nellaiappan K, Risitano A, Liu G, Nicklas G, Kagan HM. Fully processed lysyl oxidase catalyst translocates from the extracellular space into nuclei of aortic smooth-muscle cells. *J Cell Biochem*. 2000;79(4):576—582.
53. Giampuzzi M, Oleggini R, Di Donato A. Demonstration of in vitro interaction between tumor suppressor lysyl oxidase and histones H1 and H2: definition of the regions involved. *Biochim Biophys Acta*. 2003;1647(1—2):245—251.
54. Boufraqech M, Zhang L, Nilubol N, et al. Lysyl oxidase (LOX) transcriptionally regulates SNAI2 expression and TIMP4 secretion in human cancers. *Clin Cancer Res*. 2016;22(17):4491—4504.
55. Giampuzzi M, Botti G, Di Duca M, et al. Lysyl oxidase activates the transcription activity of human collagene III promoter. Possible involvement of Ku antigen. *J Biol Chem*. 2000;275(46):36341—36349.
56. Laczko R, Csiszar K. Lysyl oxidase (LOX): functional contributions to signaling pathways. *Biomolecules*. 2020;10(8):1093.